Tapered Copolymers of Styrene and 4-Vinylbenzocyclobutene via Carbanionic Polymerization for Crosslinkable Polymer Films

Daniel Leibig,[1,2†] Margarita Messerle,[3†] Tobias Johann,[1] Christian Moers,[1,2] Farzaneh Kaveh,[3] Hans-Jürgen Butt,[3] Doris Vollmer,[3] Axel H. E. Müller,[1] Holger Frey[1,2]

[1]Johannes Gutenberg-University Mainz, Institute for Organic Chemistry, D-55128, Mainz, Germany
[2]Graduate School Material Science in Mainz, Staudingerweg 9, D-55128, Mainz, Germany
[3]Max Planck Institute for Polymer Research, Ackermannweg 10, D-55128, Mainz, Germany
Correspondence to: H. Frey (E-mail: hfrey@uni-mainz.de)

Received 1 August 2019; Revised 18 September 2019; accepted 19 September 2019; published online 24 October 2019
DOI: 10.1002/pola.29515

ABSTRACT: Well-defined polystyrene homopolymers with surface-adhesive triethoxysilyl end group were synthesized via living carbanionic polymerization, epoxide end-functionalization and subsequent hydrosilylation with triethoxysilane. *Grafting-to* performance of polymers with various molecular weight (M_n = 3000–14,000 g mol^{-1}) to a silicon surface was examined in dependence of reaction time, polymer concentration, solvent and number of alkoxysilyl end groups. Crosslinkable polymers for surface modification were synthesized by statistical carbanionic copolymerization of 4-vinylbenzocyclobutene (4-VBCB) and styrene, followed by epoxide end-functionalization and triethoxysilane modification (M_n = 4000–14,000 g mol^{-1}). The copolymers were characterized by ^{1}H-NMR, THF-SEC, and matrix-assisted laser desorption and ionization time-of-flight mass spectrometry. *In situ* ^{1}H-NMR kinetic studies in cyclohexane-d_{12} provided information regarding the monomer gradient in the polymer chains, with styrene being the more reactive monomer (r_s = 2.75, $r_{4\text{-VBCB}}$ = 0.23). Thin polymer films on silicon wafers were prepared by *grafting-to* surface modification under conditions derived for the polystyrene homopolymer. The traceless, thermally induced crosslinking reaction of the benzocyclobutene units was studied by DSC in bulk as well as in 3–6 nm thick polymer films. Crosslinked films were analyzed by atomic force microscopy, ellipsometry, and nanoindentation, showing smooth polymer films with an increased modulus. © 2019 The Authors. *Journal of Polymer Science* published by Wiley Periodicals, Inc. J. Polym. Sci. **2020**, *58*, 181–192

KEYWORDS: anionic polymerization; crosslinking; kinetics; thin polymer films

INTRODUCTION In this work, we aim at a *grafting-to* method to generate coatings using polystyrene copolymers with a surface-reactive functionality at the chain end. This method relies on prefabricated, well-defined polymers with low dispersity and detailed knowledge regarding the monomer gradient structure of the polymer chains. The examination of the preparation conditions and the resulting adhesion and elasticity enables the implementation of specific surface properties, which are important for, for example, microelectronics.

Living anionic polymerization affords polymers with precisely controlled molecular weight and architecture.[1] A variety of functional groups can be introduced into these polymers using functional initiators[2,3] or various termination reagents that quantitatively terminate the living chain end.[4] With both methods, a plethora of functionalities like hydroxyl groups,[5] acidic units[6] or amino functionalities[7] is accessible. End capping of living carbanionic polymerizations using epoxides, such as ethylene oxide is a common method to introduce hydroxyl groups.[8] The termination by glycidyl ethers with protected hydroxyl groups was used by Hillmyer et al.[9] and Wang and Huang[10] in the synthesis of miktoarm star polymers. Tonhauser et al. intensively studied the termination reaction using a broad range of different glycidyl ethers with versatile functionalities, as also summarized in a review.[11,12] This strategy enables synthesis of block and

Additional supporting information may be found in the online version of this article.

†Both authors contributed equally to this work.

Dedicated to Professor Kris Matyjaszewski on the occasion of his 70th birthday.

miktoarm copolymers using ethylene oxide[13] and other monomers.[14]

In copolymers obtained by the living anionic copolymerization the materials properties depend on the distribution of both comonomers within the polymer chains. A gradient is formed when the reactivity ratios are highly disparate, that is, $r_1 \gg 1$ and $r_2 \ll 1$. Real-time ^{1}H NMR copolymerization kinetics enables the determination of reactivity ratios and thus the analysis of the comonomer distribution in the polymer chain.[15] In recent works of our group the copolymerization of styrene-derivatives with styrene and isoprene were investigated via real-time NMR measurements.[16a-f,17] A detailed understanding of the polymer microstructure is essential for applications. Currently, sequence-control of polymerizations is regarded as one of the fundamental challenges in polymer science.[18]

4-Vinylbenzocyclobutene (4-VBCB) can be polymerized by anionic[19] and radical polymerization.[20a-c,21] The cyclobutene group enables crosslinking reactions initiated by the isomerization of the cyclobutene group at around 240 °C (Scheme 1).[22,23] Copolymers of 4-VBCB prepared by radical polymerization have been used for the synthesis of particle-coil copolymers[21] and polymer brushes on nanoparticles that were subsequently crosslinked to form encapsulated nanoparticles.[24] Random copolymers and block copolymers synthesized by radical polymerization were also used in the preparation of superhydrophobic surface coatings[25] and for microelectronic applications in spin-coated films, where the crosslinking capability was used to form stable films on the surface.[26] However, to the best of our knowledge, the living anionic copolymerization of 4-VBCB with other vinyl monomers has not been studied to date.

Ultrathin polymer films can be prepared by covalent attachment of polymer brushes to a surface based on two different approaches—a *grafting-from* or *grafting-to* strategy.[27] The *grafting-from* method is the conventionally used technique to covalently attach polymer brushes onto surfaces.[28] For this purpose, living radical polymerization techniques are often used.[29] Only few *grafting-from* reactions using carbanionic vinyl polymerizations have been reported.[30] A disadvantage of the *grafting-from* strategy arises from the dispersity of molecular weight and microstructure of the synthesized polymer chains. The growing active chain ends may have different environments. Furthermore, surfaces have to be modified to carry an initiator in a separate reaction step before the polymerization.[31]

In contrast, the *grafting-to* attachment of prefabricated polymer chains onto the substrate surfaces using an active group at the chain end can be based on well-defined and fully characterized polymer chains with surface-reactive end group, albeit grafting density is commonly lower.[32] Quantitatively functionalized polymers with low dispersity can be obtained by living polymerizations. Suitable functionalities can be either introduced via the initiator or by post-polymerization modifications at the chain end. Alkoxysilanes,[33] acyl clorides,[34] but also catechols[35] may be suitable functionalities depending on the chosen surface. The attachment of surface reactive silyl groups can be achieved by hydrosilylation reactions of double bonds with the appropriate silanes.[2,12] Theoretical and quantitative descriptions of tethered polymer chains were published by de Gennes.[36] Generally two different cases can be distinguished.[37] In the case of high grafting density the distances between two neighboring anchor groups are larger than the radius of gyration. Intermolecular interactions can be neglected, and the conformation resembles those of a free chain. For small or repulsive interaction strength between the chain segments and the substrate, the conformation can be explained as mushroom-like, due to a typical random coil. The second case is the polymer brush formation induced by high grafting density and segment-segment interactions that promote polymer stretching to avoid overlap. During *grafting-to* processes transitions from mushroom conformations in a first regime to brushes in the last regime are observable.[33] Stamouli[38] and Williams[39] referred to tethered homopolymer brushes as micellar structures, because of an equilibrium of chain elasticity and surface tension of the micelles. The respective structures were observed via atomic force microscopy (AFM).[40]

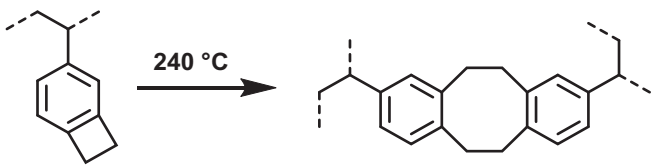

SCHEME 1 Thermal crosslinking of the 4-VBCB units.

In this contribution, we report the synthesis of well-defined polystyrene copolymers with crosslinkable benzocyclobutene groups and reactive alkoxysilyl end group for surface attachment. Thin polymer films were prepared by deposition on silicon wafers. The influence of solvent polarity, polymer concentration, number of reactive groups per polymer chain and reaction time was studied. To investigate the effect of crosslinking on thin film properties, crosslinkable poly(styrene-*co*-(4-vinylbenzocyclobutene)) P(S-*co*-(4-VBCB)) copolymers were attached onto silicon wafers. AFM, ellipsometry, and X-ray reflectivity were used to characterize the surface properties before and after thermal crosslinking (230 °C). Mechanical properties of the thin films were measured using colloidal probe (CP), AFM, and nanoindentation.

EXPERIMENTAL

Reagents

Allyl bromide (99%), allyl glycidyl ether (AGE) (>99%), methyl iodide (99%), styrene (99.5%), and 4-vinyl benzocyclobutene (97%) were purchased from Sigma-Aldrich. These reagents were cryo-transferred from CaH_2 prior to use. *sec*-Butyllithium was purchased as a 1.3 M solution in cyclohexane/hexane (92/8) by Acros Organics. Triethoxysilane (97%) was purchased from ABCR and used without further purification. Cyclohexane and THF were dried using sodium/benzophenone and cryo-transferred into the reaction vessel. Potassium naphthalide was used as a 0.5 M solution in THF. Deuterated cyclohexane-d_{12},

chloroform-d_1, and methylene chloride-d_2 were purchased from Deutero GmbH.

Instrumentation

Size-exclusion chromatography (SEC) measurements were carried out in THF on an instrument consisting of a Waters 717 plus Autosampler, a TSP Spectra Series P 100 pump, a set of three PSS-SDV 5 columns ($10^2/10^3/10^4$ Å), RI- and UV-detectors (254 nm). For calibration we used polystyrene standards provided by Polymer Standards Service. ^{1}H NMR spectra (300 and 400 MHz) and ^{13}C NMR spectra (75.5 MHz) were recorded on a Bruker AC300 or an Avance II 400. All spectra are referenced internally to the residual proton signals of the deuterated solvent. Matrix-assisted laser desorption and ionization time-of-flight (MALDI-ToF) measurements were performed on a Shimadzu Axima CFR MALDI-ToF mass spectrometer equipped with a nitrogen laser delivering 3 ns laser pulses at 337 nm. DSC measurements were performed using a Perkin Elmer DSC 7 with a Elmer Thermal Analysis Controller TAC7/DX in a temperature range from 60 to 260 °C with heating rates of 10 K min^{-1} under nitrogen unless otherwise stated.

Polystyrene-Allyl glycidyl ether; PS-AGE (1)

Vacuum-distilled styrene (10.0 mL, 87.4 mmol) was dissolved in 50 mL dry and degassed cyclohexane and cooled down to 0 °C. The corresponding amount of *sec*-butyllithium (1.3 M, 2.3 mL, 3.0 mmol) was added with a gas tight syringe and the orange-colored reaction mixture was stirred 20 h at room temperature. AGE (1.8 mL, 15 mmol, 5 equiv.) was introduced with a syringe and the orange color disappeared immediately. The solution was stirred for additional 20 h. After concentrating in vacuum, the reaction mixture was precipitated several times in methanol to obtain PS-AGE. Pure end-functionalized polystyrene was obtained using flash chromatography (stationary phase: silica; eluent 1: toluene (for PS-OH); eluent 2 THF (for PS-AGE); $R_{f,THF}$ = 0.1). The purification is performed by first elution of the non-functionalized PS-OH using toluene as eluent. After separation of this side product, pure PS-AGE is obtained by further elution with THF.[10] Yield: 75%. ^{1}H NMR (300 MHz, $CDCl_3$, δ in ppm) (Fig. S3): 7.55–6.25 (PS aromatic), 6.00–5.75 (1H, C*H*═CH_2), 5.35–5.05 (2H, CH═CH_2), 4.00–3.80 (2H, CH_2—CH═CH_2), 3.60–2.90 (3H, AGE C*H*-CH_2), 2.60–0.82 (PS backbone), 0.82–0.55 (6H, init CH_3); Fig. S12 shows a typical MALDI-ToF of PS_{30}-AGE.

PS-AGE-Methyl (2)

2.5 g (0.77 mmol) of PS-AGE was dissolved in dry THF and titrated with potassium naphthalide in THF (0.5 M) until the green color remained. 0.72 mL methyl iodide, MeI, (12 mmol, 15 equiv.) was added with a syringe, the green color disappeared and the solution became cloudy. After stirring for 1 h at room temperature, the solvent was removed under reduced pressure and the residue was dissolved in chloroform and precipitated twice in methanol. Yield: 94%. ^{1}H NMR (300 MHz, $CDCl_3$, δ in ppm) (Fig. S4): 7.55–6.25 (PS aromatic), 6.00–5.75 (1H, C*H*═CH_2), 5.35–5.05 (2H, CH═CH_2), 4.00–3.80 (2H, CH_2—CH═CH_2), 3.60–2.90 (6H, AGE C*H*—CH_2, O—CH_3), 2.60–0.82 (PS backbone), 0.82–0.55 (6H, init CH_3).

PS-AGE-Allyl (3)

2.3 g (0.71 mmol) of PS-AGE was dissolved in dry THF and titrated with potassium naphthalide in THF (0.5 M) until the green color remained. 1.2 mL allyl bromide (14 mmol, 20 equiv.) was added with a syringe and the green color disappeared. After stirring for 3 h at room temperature, the solvent was removed under reduced pressure and the residue was dissolved in chloroform and precipitated twice in methanol. Yield: 96%. ^{1}H NMR (300 MHz, $CDCl_3$, δ in ppm) (Fig. S5): 7.55–6.25 (PS aromatic), 6.00–5.75 (2H, C*H*═CH_2), 5.35–5.05 (4H, CH═CH_2), 4.00–3.80 (4H, CH_2—CH═CH_2), 3.60–2.90 (3H, AGE C*H*—CH_2, O—CH_3), 2.60–0.82 (PS backbone), 0.82–0.55 (6H, init CH_3).

PS-TEOS-Methyl (4)

1.95 g (0.60 mmol) PS-AGE-Methyl was dissolved in chlorobenzene, Karstedt's catalyst (2 μL) and triethoxysilane (TEOS) (1.1 mL, 10 equiv.) were added and the reaction mixture was stirred 72 h at 60 °C. The solvent was removed *in vacuo* and the residue was dissolved in methylene chloride and precipitated in methanol. Yield: 87%. ^{1}H NMR (300 MHz, CD_2Cl_2, δ in ppm) (Fig. S6): 7.55–6.25 (PS aromatic), 3.60–2.90 (O—C*H*, O—CH_3, O—CH_2), 2.60–0.82 (PS backbone, O—CH_2—CH_3), 0.82–0.55 (8H, init CH_3, CH_2—Si).

PS-TEOS$_2$ (5)

2.3 g (0.68 mmol) PS-AGE-Allyl was dissolved in chlorobenzene, Karstedt's catalyst (2 μL) and TEOS (1.9 mL, 15 equiv.) were added and the reaction mixture was stirred 72 h at 60 °C. The solvent was removed *in vacuo* and the residue was dissolved in methylene chloride and precipitated in methanol. Yield: 93%. ^{1}H NMR (300 MHz, CD_2Cl_2, δ in ppm) (Fig. S7): 7.55–6.25 (PS aromatic), 3.60–2.90 (O—C*H*, O—CH_2), 2.60–0.82 (PS backbone, O—CH_2—CH_3), 0.82–0.55 (10H, init CH_3, CH_2—Si).

P(S-*co*-(4-VBCB))-AGE (6)

Vacuum-distilled styrene (1.50 mL, 13 mmol) and fresh distilled 4-VBCB (0.31 mL, 2.3 mmol) were dissolved in 40 mL dry and degassed cyclohexane and cooled down to 0 °C. The corresponding amount of *sec*-butyllithium (1.3 M, 0.31 mL, 0.41 mmol) was added with a gas tight syringe and the orange-colored reaction mixture was stirred 20 h at room temperature. AGE (0.72 mL, 6.1 mmol, 15 equiv.) was introduced with a syringe and the orange color disappeared immediately. The solution was stirred for additional 20 h. After concentrating in vacuum, the reaction mixture was precipitated several times in methanol to obtain P(S-*co*-(4-VBCB))-AGE. Pure end-functionalized polymer was obtained using flash chromatography techniques[10] analogous to the described procedure for PS-AGE (stationary phase: silica; eluent 1: toluene [for P(S-*co*-(4-VBCB))]; eluent 2 THF (for P(S-*co*-(4-VBCB))-AGE); $R_{f,THF}$ = 0.1). Yield: 80%. ^{1}H NMR (400 MHz, $CDCl_3$, δ in ppm) (Fig. S8): 7.55–6.25 (PS aromatic), 6.00–5.75 (1H, C*H*═CH_2), 5.35–5.05 (2H, CH═CH_2), 4.05–3.80 (2H, CH_2—CH═CH_2), 3.75–2.90 (AGE C*H*—CH_2, 4-VBCB CH_2—CH_2), 2.60–0.82 (backbone), 0.82–0.55 (6H, init CH_3); Figure S9. ^{13}C NMR spectrum of P(S-*co*-(4-VBCB))-AGE in $CDCl_3$.

P(*S-co*-(4-VBCB)-AGE-Methyl (7)
The synthesis was equivalent to the preparation of PS-AGE-Methyl (Fig. S10).

P(*S-co*-(4-VBCB)-TEOS-Methyl (8)
The synthesis was similar to the preparation of PS-TEOS-Methyl (Fig. S11).

***Grafting-to* process**
Polymer was dissolved in dry toluene or DCM and 1.2 vol % TEA was added. The solution was stirred for 1 h and filtered through a PTFE filter with a pore size of 0.25 μm. A silicon wafer was heated in a 1:1:10 mixture of ammonia solution (25%), hydrogen peroxide solution (35%), and MilliQ water at 80–85 °C to ensure a homogeneous oxidation of the surface. The silicon wafer was immersed in the reaction mixture and gently swirled for 1–24 h. After the grafting reaction, the samples were washed by three times repeated shaking in 5 ml of filtrated solvent to rinse off physisorbed chains. They were further washed with filtrated ethanol and dried under a nitrogen flow.

RESULTS AND DISCUSSION

End-Functionalized Polystyrenes

End-functionalized polystyrene homopolymers **(1)** were obtained in high yields using an established synthetic approach (Scheme 2).[12] The molecular weights were between 3000 and 13,500 g mol^{-1} with dispersities $Đ$ < 1.15. The end-functionalized polystyrenes were purified by column chromatography with toluene as an eluent to remove a fraction containing mainly proton-terminated (i.e., non-functionalized) polystyrene.[41] Polystyrene with an allyl glycidyl ether end group shows a longer retention time on silica due to the polar character of the hydroxyl group. This effect decreases with increasing chain and is limited to molecular weights up to 15,000 g mol^{-1}. PS-AGE was characterized by ^{1}H NMR spectroscopy and SEC (Figs. S1 and S3, Table 1). MALDI-ToF mass spectrometry was utilized to evaluate the degree of functionalization and the efficiency of the subsequent modification (Fig. S12). In a second step, the free hydroxyl group at the chain end was modified with a methyl group **(2)** and an allyl group **(3)**, respectively, to prepare polymers with either one or two double bonds at the chain end. Successful conversion was verified by ^{1}H NMR spectroscopy as the proton signal in α-position to the hydroxyl group disappeared (δ = 3.56 ppm) (Fig. S4). MALDI-ToF MS also confirmed

TABLE 1 Characterization Data for PS_x-AGE Measured by SEC and ^{1}H NMR Spectroscopy

Polymer	$M_{n,NMR}$ (g mol^{-1})	$M_{n,SEC}$ (g mol^{-1})	$Đ_{SEC}$
PS_{30}-AGE	3290	3250	1.08
PS_{42}-AGE	4510	4360	1.15
PS_{48}-AGE	5170	5580	1.15
PS_{80}-AGE	8400	9640	1.06
PS_{114}-AGE	11850	13400	1.05

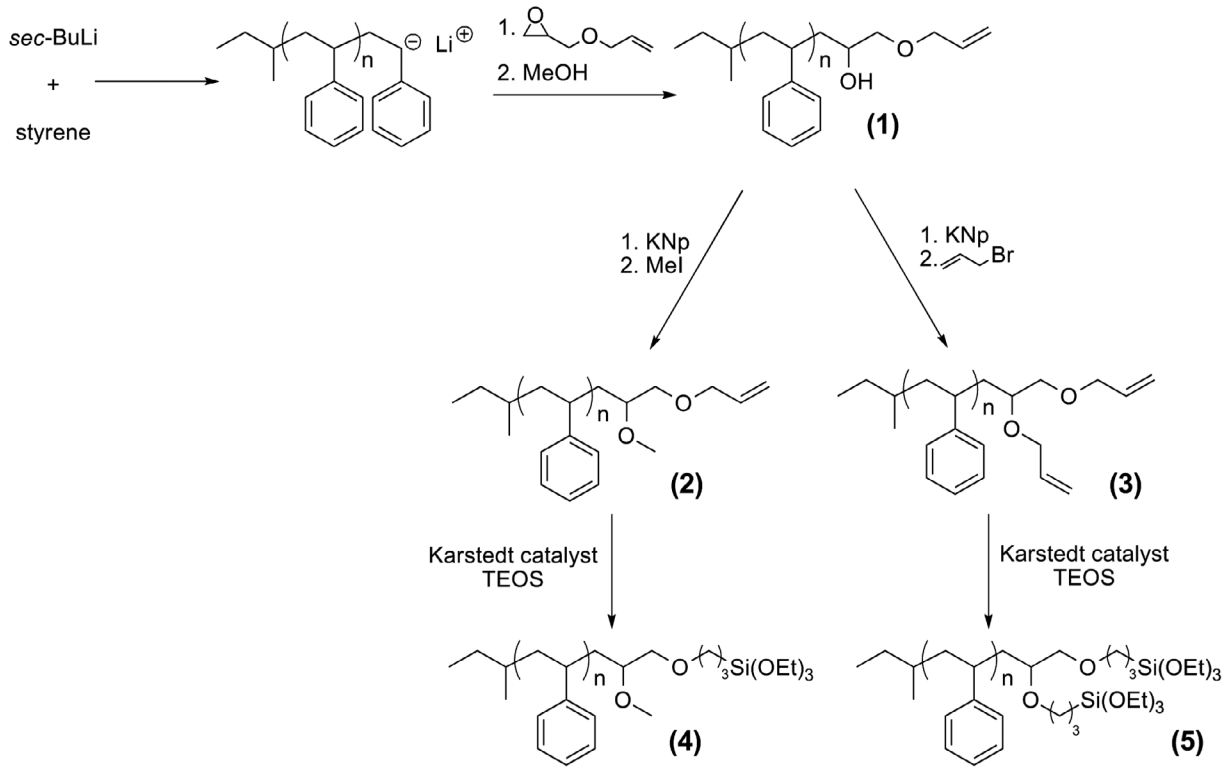

SCHEME 2 Synthesis of end-functionalized polystyrene and post-polymerization functionalization of the end group.

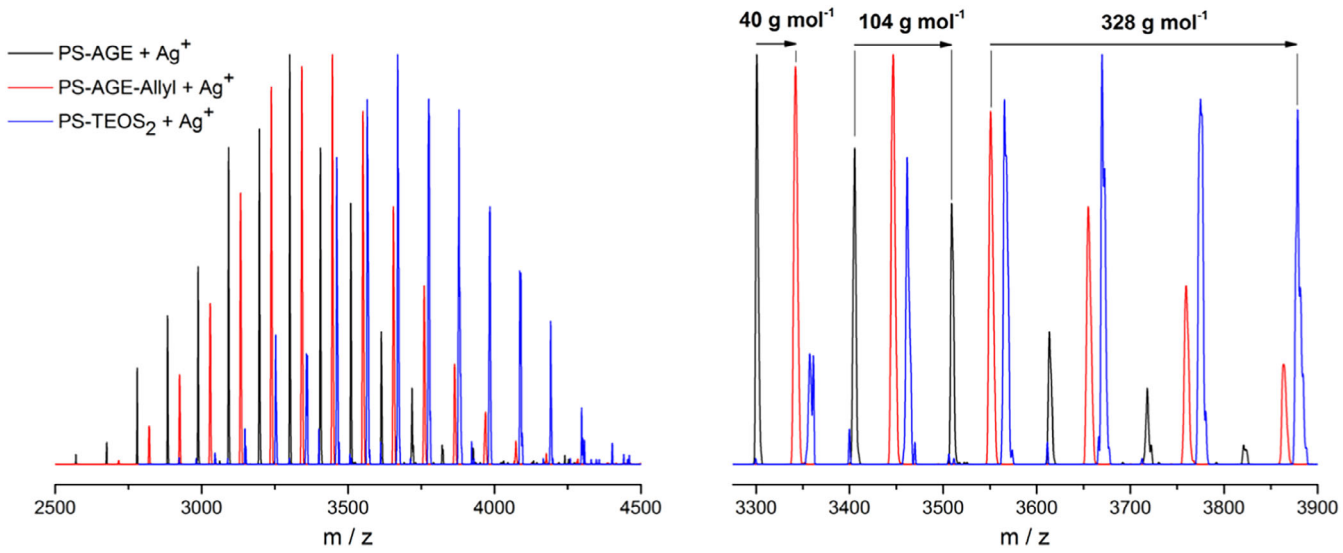

FIGURE 1 Left: MALDI-ToF MS spectrum of PS_{30}-AGE (black), PS_{30}-AGE-Allyl (red), and PS-$TEOS_2$ (blue); right: Shift of the polymer signals by 40 g mol^{-1} (junction of the allyl-group), the distance between styrene repeating units 104 g mol^{-1} and the shift of 328 g mol^{-1} (insertion of two $HSi(OEt)_3$ end groups).

quantitative modification (Figs. S13 and S15). Figure 1 shows an overlay of three MALDI-ToF MS spectra of the AGE-terminated polystyrene (black), the post-polymerization modified polystyrene with two terminal double bonds (PS-AGE-Allyl, red) and the polymer after an additional hydrosilylation reaction of both double bonds with triethoxysilane (PS-$TEOS_2$, blue).

In a third step, the interacting end group was introduced by hydrosilylation with TEOS using the Karstedt catalyst. Quantitative conversion after 3 days reaction time was verified by MALDI-ToF mass and ^{1}H NMR analysis (Figs. S6, S7, S14, and S16). Absence of signals of the starting material in MALDI-ToF MS spectra as well as complete disappearance of the double bond signals in ^{1}H NMR confirmed quantitative end group modification. Consequently, this method is suitable to synthesize polymers with varying chain lengths, while controlling the number of end groups that can react with a surface.

Thin Films of TEOS End-Functionalized Polystyrene

The two alkoxysilyl-functional polymers PS_{30}-TEOS and PS_{42}-TEOS both yielded a mean film thickness of d = 3.2 ± 0.3 nm, as measured by ellipsometry (Fig. 2). Their film thickness was constant after less than 1 h surface treatment. Higher molecular weights, M_n = 9640 and 13,400 g mol^{-1} lead to thicker films with d = 5.1 ± 0.5 nm and d = 5.6 ± 0.3 nm after 24 h. These results show fast coverage of the surface with tethered chains in case of low-molecular-weight polymers. Polymers with higher molecular weight are subject to thermodynamic

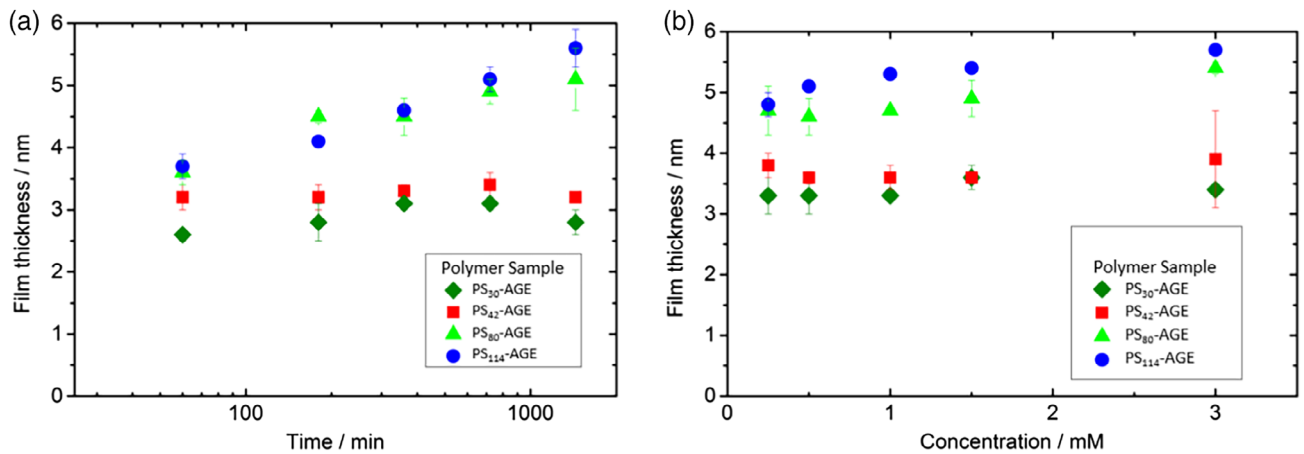

FIGURE 2 (a) Film thickness measured by ellipsometry versus reaction time (1–24 h) of *grafting-to* in solution for PS-TEOS-Me of different molecular weights in toluene, $c \approx 1$ mM; (b) Film thickness and concentration of the grafting solutions for different molecular weight in toluene, c = 0.25–3 mM, t = 24 h.

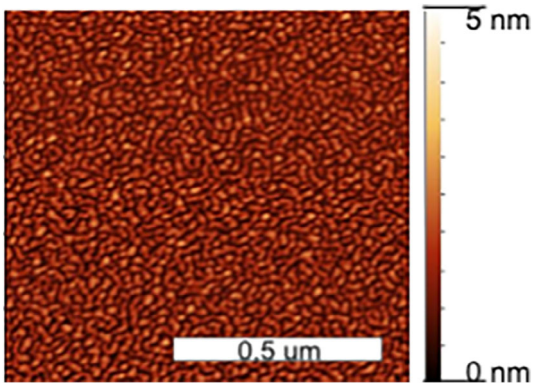

FIGURE 3 1 μm^2 AFM height image of a PS-TEOS-Me (M_n = 13,400 g mol^{-1}) coated silicon wafer; *grafting-to* from toluene solution, t = 24 h, c = 1 mM.

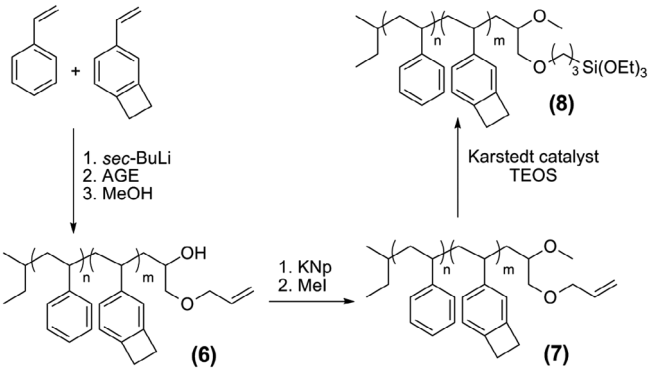

SCHEME 3 Synthesis and post-polymerization reaction of P(S-*co*-(4-VBCB)) copolymers.

and kinetic inhibition of the grafting reaction, caused by more hindered diffusion of free chains through already tethered brushes to the substrate surface.

Polymers with molecular weights of M_n = 3250–4360 g mol^{-1} exhibited no significant dependence of the film thickness on concentration [Fig. 2(b)]. The mean values were d = 3.4 ± 0.1 nm (M_n = 3250 g mol^{-1}) and d = 3.7 ± 0.1 nm (M_n = 4360 g mol^{-1}). Film thicknesses of high-molecular-weight polymers are d (PS_{80}-TEOS-Me) = 4.7 ± 0.4 nm and d (PS_{114}-TEOS-Me) = 4.8 ± 0.2 nm for low concentrations of 0.5 mM with a slight increase with increasing concentration.

Using AFM, we investigated the topography of the films. AFM shows that the reaction results in a complete coverage of the surface. A silicon wafer coated with polymers of M_n = 13,400 g mol^{-1} is shown in the AFM height image (Fig. 3). The surface of this film obtained at 1 mM polymer concentration has a thickness d = 5.3 ± 0.1 nm and shows a low roughness of *RMS* = 0.53 nm. For concentrations exceeding 1 mM, less rough films were observed, potentially due to slight stretching of chains when more chains were grafted (Fig. S22).

Thin film characterization showed that the use of end-functional polystyrene with two TEOS end groups did not result in higher film thicknesses, that is, d (PS_{42}-$(TEOS)_2$) = 3.0 ± 0.3 nm. Therefore, thin crosslinkable polystyrene films shown below were prepared with only one TEOS end functionality.

Synthesis of Thermally Crosslinkable Polystyrene Copolymers

Copolymerization of styrene and 4-VBCB and subsequent termination with AGE permits to prepare crosslinkable copolymers that can be covalently attached to a surface after TEOS end functionalization. In analogy to PS-AGE also statistical P(S-*co*-(4-VBCB))-AGE copolymers with molecular weights between 4000 and 14,000 g mol^{-1} with low dispersities were synthesized at room temperature, both in THF and cyclohexane (Scheme 3 and Table 2). The copolymers were also purified by column chromatography to remove the unfunctionalized polymer chains (5%–10%). Molar masses were determined by SEC and ^{1}H NMR spectroscopy showing successful end functionalization. MALDI-ToF characterization confirms the incorporation of both monomers into the polymer chains (Fig. S17). The incorporated amount of the comonomer 4-VBCB was determined by ^{1}H NMR spectroscopy via comparison of the initiator integral (δ = 0.55–0.88 ppm), the integral of the four protons at the cyclobutene ring (δ = 2.90–3.75 ppm), and the integral of the aromatic protons (δ = 6.25–7.55 ppm) of the PS moieties. The 4-VBCB content used in the starting monomer feed was also found in the final copolymer composition. Polymers with contents of 4-VBCB between 3 and 20 mol % were prepared.

It is an intriguing question, whether the cyclobutene substituent significantly influences the monomer reactivity in the copolymerization of styrene and 4-VBCB. In this respect, real-time ^{1}H NMR kinetics was conducted under reaction conditions in the NMR tube equivalent to those of the polymer synthesis in batch. Deuterated cyclohexane was used as a solvent. The decrease of the integrals of the double bond signals of styrene (δ (ppm) = 5.62 (dd, J = 17.6, 1.1 Hz), 5.10 (dd, J = 11.0, 1.1 Hz)) and 4-VBCB (δ (ppm) = 5.55 (dd, J = 17.6, 1.2 Hz), 5.02 (dd, J = 10.8, 1.2 Hz)) is equivalent to the single monomer conversion. The polymerization of an equimolar mixture of the comonomers was initiated by addition of *sec*-BuLi via a syringe in the NMR tube, and the reaction was monitored by real time ^{1}H NMR spectroscopy at 400 MHz. With increasing reaction time, a decrease of the well-resolved monomer signals was observed as well as an increase of the broad polymer signals (Fig. S19). The relevant part for the real-time ^{1}H NMR kinetics is the double bond region shown in Figure 4. The styrene signal (highlighted in red) decreases faster than the 4-VBCB vinyl bond signals (highlighted in blue).

The data obtained by NMR can be transferred into a graph correlating the single monomer conversion with total conversion [Fig. 5(a)]. The resulting diagrams allow determination of the

TABLE 2 Properties of the Synthesized P(S_x-*co*-(4-VBCB)$_y$)-AGE Copolymers

Polymer	Solvent	4-VBCB content (mol %)	$M_{n,NMR}$ (g mol^{-1})	$M_{n,SEC}$ (g mol^{-1})	$Đ$
P(S_{40}-*co*-(4-VBCB)$_{1.5}$)-AGE	THF	3.6	4560	4400	1.24
P(S_{56}-*co*-(4-VBCB)$_{2.6}$)-AGE	CH	4.5	6300	6490	1.06
P(S_{49}-*co*-(4-VBCB)$_{11}$)-AGE	THF	18	6670	6710	1.07
P(S_{57}-*co*-(4-VBCB)$_{9.4}$)-AGE	CH	14	7290	7480	1.08
P(S_{94}-*co*-(4-VBCB)$_{3.9}$)-AGE	CH	3.8	10,850	11,300	1.05
P(S_{92}-*co*-(4-VBCB)$_{23}$)-AGE	CH	20	13,300	13,600	1.08

copolymer microstructure and the corresponding reactivity ratios. As a first result, styrene is incorporated faster than 4-VBCB. This leads to a gradient structure with higher styrene content at the start of the polymer chains and a chain end consisting predominantly of crosslinkable 4-VBCB units. The data were fitted via by using the Meyer-Lowry formalism, and reactivity ratios were determined to be r_s = 2.75 and $r_{4\text{-VBCB}}$ = 0.23 (Fig. S20).[42] While the methylene group in meta position shows no significant influence with respect to charge distribution, the methylene group in para-position gives a positive inductive effect to the monomer. Similar results were obtained in the copolymerization of 4-methylstyrene with styrene (r_s = 2.62 and $r_{4\text{-MS}}$ = 0.37).[17] Thus, 4VBCM is less reactive than styrene. The time conversion plot of the reaction kinetics in Figure 5 (b) visualizes the significantly slower reaction of the functional 4-VBCB comonomer.

An important feature of 4-VBCB is its ability to undergo crosslinking reactions at elevated temperatures by reaction of the cyclobutene rings to a bridged cyclooctane ring system (Scheme 1). Crosslinking proceeds by a [4 + 2]-cycloaddition.[43] The formation of crosslinked polymers leads to a decrease of the flexibility of the polymer chains, increasing the glass transition temperature, T_g. Crosslinking at 240 °C of a polymer containing 3.6% of 4-VBCB led to a maximum increase of the T_g from 76 to 86 °C, demonstrating that no network was formed with this low content of 4-VBCB units. A content of the crosslinkable comonomer of 4.5% causes an even more significant ΔT_g of 17 °C because of the higher degree of crosslinking (Fig. S18). For polymers exceeding 10% of 4-VBCB, no T_g was observable after thermal treatment due to the high degree of crosslinking. These results agree with the data of Sakellariou et al. for homopolymers based on 4-VBCB.[22]

The time for the crosslinking reaction is important in view of applications of the copolymers. To determine this parameter, the dependence of ΔT_g on the reaction time was investigated using bulk samples. To determine the time interval required to obtain full crosslinking for a given copolymer sample, a series of DSC experiments was performed. Polymer samples with identical chain length and 4-VBCB-content were heated rapidly (100 °C min^{-1}) to 240 °C, and the samples were kept at this temperature for different time intervals ranging from 30 s to 30 min. Subsequently, the sample was cooled to 40 °C and the T_g of the polymer was measured again. With increasing heating period, the observed T_g gradually increased until a plateau was reached after 20 min (Fig. 6). Increasing T_gs correspond to an increasing degree of crosslinking of the samples. Thus, full conversion of the cycloaddition reaction for gradient copolymers in bulk with a low content of 4-VBCB is achieved after 20 min reaction time at 240 °C. Additional proof of conversion is obtained via ^{1}H NMR spectroscopy, as the signal of the cyclobutene group at 3.20 ppm disappeared. As expected, only the copolymer with 3.6% content of 4-VBCB was soluble after the crosslinking reaction, due to the presence of merely one crosslinkable 4-VBCB group per chain on average.

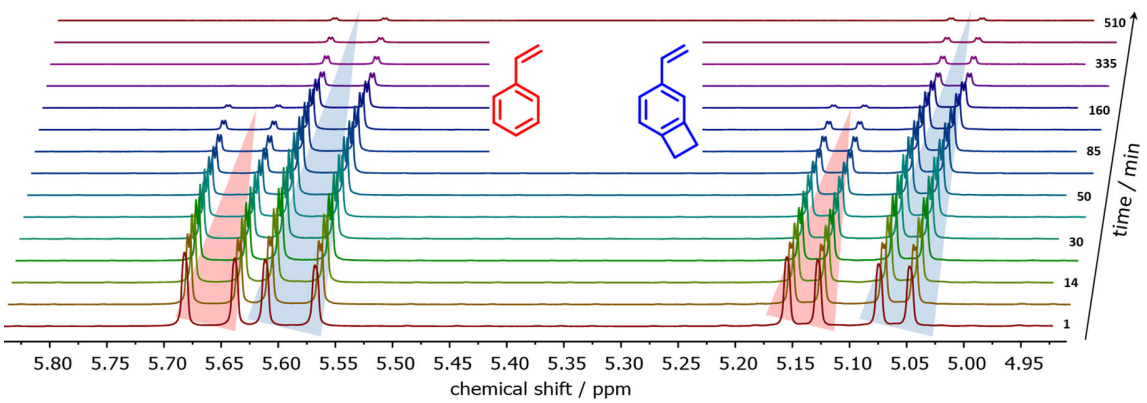

FIGURE 4 ^{1}H NMR spectrum in cyclohexane-d_{12} at room temperature, showing the signals of the double bonds of styrene (red) and 4-VBCB (blue) versus time.

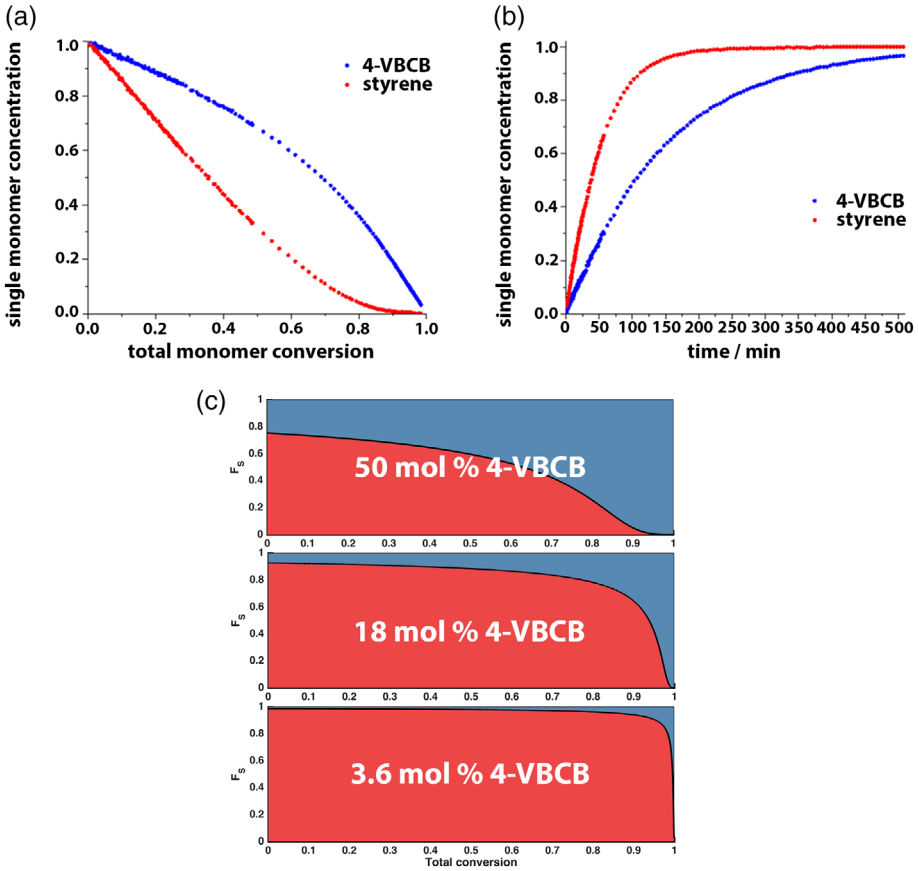

FIGURE 5 (a) Single monomer concentrations of styrene (red) and 4-VBCB (blue) in cyclohexane-d_{12} versus the total conversion; (b) Plot of the single monomer conversions of styrene (red) and 4-VBCB (blue) versus time at room temperature. (c) Gradient structure of the copolymers at equimolar ratio, 18 and 3.6 mol % 4-VBCB content.

Ultrathin Crosslinkable Polymer Films

Crosslinking in ultrathin films of the copolymers was investigated by AFM. Two different samples of P(S-*co*-(4-VBCB))-TEOS-Me were used: a copolymer with 3.6% (for comparison) and another with 18% of crosslinkable units. Six polymer films were prepared, each with optimized reaction conditions (see Supporting Information) in 1 mM toluene solutions and 24 h reaction time. Film thicknesses were measured by ellipsometry, as described above (Table 3).

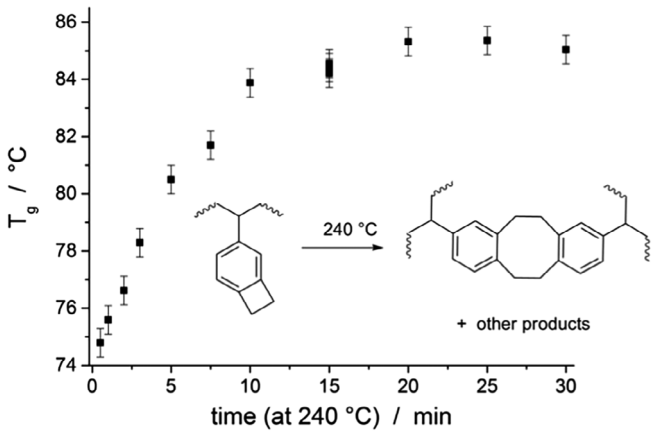

FIGURE 6 Dependence of the T_g on the crosslinking time of P(S-*co*-(4-VBCB))-AGE, reaction temperature 240 °C (3.6% 4-VBCB moieties).

Directly after formation, homogeneous polymer films with low roughness of RMS = 0.48 nm were observed by AFM, irrespective of the crosslink density [Fig. 7(a,d)]. When annealing the films to 240 °C for 90 min, the roughness significantly increased to RMS = 0.8–1.3 nm [Fig. 7(b,e)]. After a heating period of 3 h the roughness decreased slightly [Fig. 7 (c,f)]. No difference could be detected by AFM between ultrathin film samples with 3.6% and 18% of crosslinkable benzocyclobutene groups. Dewetting or microcrack formation was never observed.

A tentative explanation for this behavior is provided by the reaction kinetics discussed before. The results of copolymerization kinetics showed a gradient of incorporation for the benzocyclobutene groups over the whole chain. As a consequence of their reactivity the density of crosslinkable units in the neighborhood of the anchor group is higher than at the

TABLE 3 Results of Ellipsometry and AFM Measurements on Ultrathin Films on Silicon

	$P(S_{40}$-*co*-$(4\text{-VBCB})_{1.5})$-AGE (3.6% 4-VBCB)		$P(S_{49}$-*co*-$(4\text{-VBCB})_{11})$-AGE (18% 4-VBCB)	
Method	d/nm	RMS/nm	d/nm	RMS/nm
24 h after grafting-to in toluene solution	3.3 ± 0.1	0.48	4.2 ± 0.2	0.48
Heated for 90 min at 240 °C, 24 h after grafting	4.0 ± 0.1	1.10	3.3 ± 0.1	1.27
Heated for 180 min at 240 °C, 24 h after grafting	3.1 ± 0.1	0.84	3.8 ± 0.2	0.47

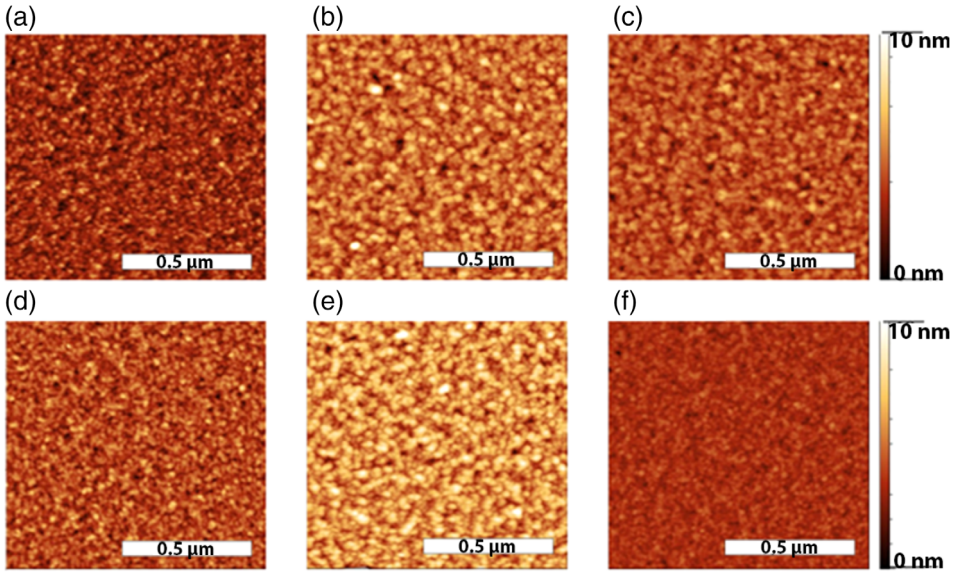

FIGURE 7 AFM comparison of films with 3.6 (a–c) and 18% (d–f) crosslinker. (a,d) measured directly after 24 h *grafting-to* in toluene solution and subsequent drying overnight in vacuum. (b,e) heated 90 min at 240 °C after 24 h *grafting-to* in toluene solution. (c,f) Heated for 180 min at 240 °C after 24 h *grafting-to* in toluene solution.

chain end. After surface grafting of the polymer chains these groups are close to the substrate, leading to preferential crosslinking in the interface layer at the Si wafer.

Figure 8(a) shows an AFM adhesion force map and a selected force-distance curve of a P(S-*co*-(4-VBCB))-TEOS film containing 18% crosslinkable groups after heating at 240 °C for 3 h. In addition to the brightness gradient that corresponds to a force gradient, a variation of the surface roughness could be observed. The blue line in Figure 8 (b) represents the engaging of the CP. A snap-into-contact at a small distance of 2 nm to the surface results from Van der

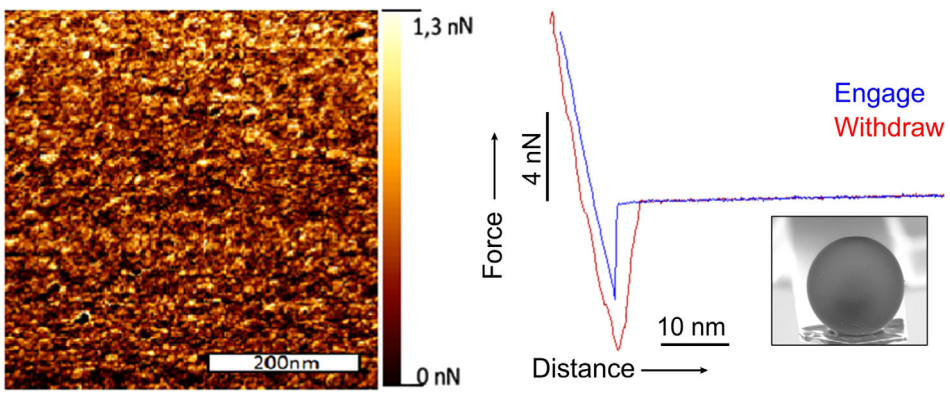

FIGURE 8 Left: AFM force map of a P(S-*co*-(4-VBCB))-TEOS-film with 18% copolymer (grafting reaction in toluene, M_n = 6710 g mol^{-1}, c = 0.84 mM, t = 24 h, d = 3.8 ± 0.2 nm) after heating at 240 °C for 180 min; right: Force–distance curve with the engaging curve in blue and retraction curve in red. SEM image of the used colloidal probe tip with 16.3 µm radius.

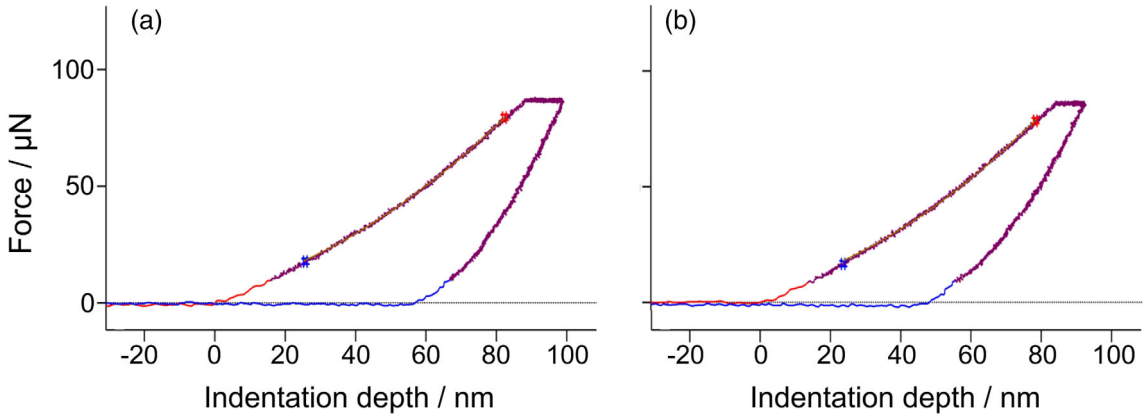

FIGURE 9 Measurement of a P(S-*co*-(4-VBCB))-TEOS-film with M_n = 13,400 g mol^{-1} and 18% copolymer direct after the reaction (b) and after 3 h of heating at 240 °C (c)

Waals forces. The red line describes the withdrawing by an adhesion force of round about 6 nN. The maximum difference of the adhesion forces was 1.3 nN. The mean force of adhesion of all measured surfaces was F_{adh} = 6.0 ± 0.1 nN and no change during the crosslinking process was observable. This observation indicates that homopolymers and copolymers had similar surface energies. The results were confirmed by CP AFM measurements.

Nanoindentation measurements with a maximum applied force of 80 µN between the measured film sample and the indentation tip were carried out as well. The force time program defined an approach of the tip to the surface at a rate of 16 µN s^{-1} within 5 s, until the maximum of 80 µN was reached. The force was applied for 5 s. Then, the tip was retracted again at a rate of 16 µN s^{-1} for 5 s. In each case, four measurements were performed on one polymer film of the same heating period and averaged over the resulting elasticity modules. First, samples were measured without crosslinkable groups. Indentation curves of the crosslinkable P(S-*co*-(4-VBCB)) films showed less flow as compared to pure polystyrene. The shape of the measured curves offered a typical visco-elasto-plastic behavior (Fig. 9).

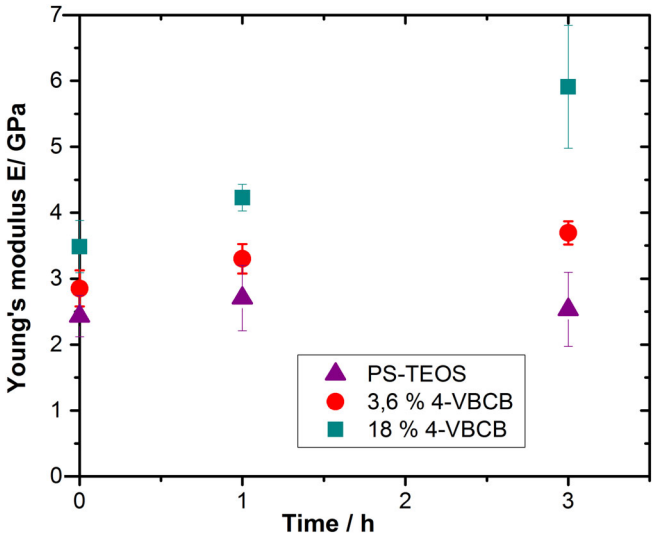

FIGURE 10 Young's modulus in dependence of heating time; violet triangles: PS-TEOS (M_n = 4360 g mol^{-1}); red circles: P(S-*co*-(4-VBCB))-TEOS-Me (M_n = 4400 g mol^{-1} and 3.6% copolymer); green squares: P(S-*co*-(4-VBCB))-TEOS-Me (M_n = 6710 g mol^{-1} and 18% copolymer)

Figure 9 shows a glass-like behavior in the graph of a P(S-*co*-(4-VBCB))-TEOS film with M_n = 13,400 g mol^{-1} and a percentage of 18% of crosslinkable groups after 3 h heating. Parallel curves of approaching and withdrawing are typical for glasses. Less creeping in comparison to measurements after 1 h of heating was observed, in line with reduced viscous properties caused by an advanced crosslinking of the polymer chains. The Young's modulus of the samples was calculated by the Nanoindenter Software using the Hertz Model under respect of the measuring points between the chosen blue and red set points.

The Young's modulus of unheated samples was E = 2.9 ± 0.6 GPa (10). The differences in the unheated samples resulted from increasing molecular weights of PS-TEOS over P(S-*co*-(4-VBCB))-TEOS-Me 3.6% to P(S-*co*-(4-VBCB))-TEOS-Me 18%. The magnitude of the resulting modulus corresponds to the literature values.[44] After a heating period of 3 h, the sample of high copolymer percentage showed a strong increase in the modulus to E = 5.9 ± 0.9 GPa (Figure 10).

CONCLUSIONS

Anionic polymerization was employed to generate well-defined polystyrenes with surface-reactive triethoxysilane end groups for surface coatings by covalently bonded films on substrates like silicon. This concept was extended to the carbanionic copolymerization of styrene with 4-VBCB both in cyclohexane and THF. The reactivity ratios in cyclohexane were measured by real-time ^{1}H NMR kinetics in cyclohexane. Based on the Meyer-Lowry formalism r_S = 2.75 and $r_{4\text{-VBCB}}$ = 0.23 were determined, showing a gradient structure with higher density of 4-VBCB units at the chain end. The chain end was further reacted with

allyl glycidyl ether and subsequently hydrosilated to carry triethoxysilyl groups.

Using the *grafting-to* technique in toluene, both the polystyrene as well as the gradient copolymer chains were coated onto silicon wafers. The dependence of the film thickness on molecular weight, polymer concentration and reaction time were studied using functionalized polystyrene chains. Above a concentration of 0.2 mM 3–6 nm thick films were obtained. The concentration did not change film thickness sensitively. For the higher molecular weight polymers (M_n = 9640 and 13,400 g mol^{-1}), the film thickness increased with time up to 24 h. For low-molecular-weight polymers (M_n = 3250 g mol^{-1}), the final film thickness of 3 nm was already achieved after 1 h. Polymers with a molecular weight of M_n = 13,400 g mol^{-1} in 3 mM toluene solutions and reaction times of 24 h showed the highest film thickness (d = 5.4 $\pm$ 0.2 nm) and roughness (RMS = 0.76 nm on 1 μm^2).

The time required for thermal crosslinking process of the 4-VBCB units in bulk at 240 °C was determined. Complete conversion was observed within 20 min. The end-functionalized polymers were grafted onto silicon surfaces under optimized preparation conditions. Also, surface-bonded P(S-*co*-(4-VBCB)) can be crosslinked. Film thickness, topography, and adhesion did not change by crosslinking, but the Young's modulus measured by nanoindentation strongly increased with the amount of crosslinkable 4-VBCB groups. CP techniques showed that the Young's modulus of the crosslinked films almost doubled as compared with the uncrosslinked films. In summary, we demonstrate a traceless method to prepare ultrathin, homogeneous, and hard polymer coatings for silicon wafers of P(S-*co*-(4-VBCB).

ACKNOWLEDGMENTS

D.L. and C.M. acknowledge a fellowship through the Excellence Initiative (DFG/GSC 266) in the context of MAINZ "Materials Science in Mainz". We thank E. Berger-Nicoletti, M. Müller, M. Schmelzer, S. Geiter, U. Rietzler, G. Schäfer, and G. Auernhammer for technical support and stimulating discussions.

References and Notes

1 D. Baskaran, A. H. E. Müller, *Prog. Polym. Sci.* **2007**, *32*, 173.

2 R. P. Quirk, V. Chavan, J. Janoski, A. Yol, C. Wesdemiotis, *Macromol. Symp.* **2013**, *323*, 51.

3 a) R. P. Quirk, S. Sahoo, *Macromol. Symp.* **2013**, *325-326*, 77. b) I. Lee, F. S. Bates, *Macromolecules* **2013**, *46*, 4529.

4 R. P. Quirk, D. L. Gomochak, *Rubber Chem. Technol.* **2003**, *76*, 812.

5 D. H. Richards, M. Szwarc, *Trans. Faraday Soc.* **1959**, *55*, 1644.

6 R. P. Quirk, J. Yin, L. J. Fetters, *Macromolecules* **1989**, *22*, 85.

7 K. Ueda, A. Hirao, S. Nakahama, *Macromolecules* **1990**, *23*, 939.

8 a) R. P. Quirk, J.-J. Ma, *J. Polym. Sci. Part A: Polym. Chem.* **1988**, *26*, 2031. b) R. P. Quirk, R. T. Mathers, C. Wesdemiotis, M. A. Arnould, *Macromolecules* **2002**, *35*, 2912.

9 Z. Li, M. A. Hillmyer, T. P. Lodge, *Macromolecules* **2004**, *37*, 8933.

10 G. Wang, J. Huang, *J. Polym. Sci. Part A: Polym. Chem.* **2008**, *46*, 1136.

11 a) C. Tonhauser, H. Frey, *Macromol. Rapid Commun.* **2010**, *31*, 1938. b) C. Tonhauser, D. Wilms, F. Wurm, E. B. Nicoletti, M. Maskos, H. Löwe, H. Frey, *Macromolecules* **2010**, *43*, 5582. c) C. Tonhauser, B. Obermeier, C. Mangold, H. Löwe, H. Frey, *Chem. Commun.* **2011**, *47*, 8964.

12 C. Tonhauser, A. A. Golriz, C. Moers, R. Klein, H.-J. Butt, H. Frey, *Adv. Mater.* **2012**, *24*, 5559.

13 a) A. Natalello, C. Tonhauser, E. Berger-Nicoletti, H. Frey, *Macromolecules* **2011**, *44*, 9887. b) C. Tonhauser, M. Mazurowski, M. Rehahn, M. Gallei, H. Frey, *Macromolecules* **2012**, *45*, 3409.

14 J. Morsbach, A. Natalello, J. Elbert, S. Winzen, A. Kroeger, H. Frey, M. Gallei, *Organometallics.* **2013**, *32*, 6033.

15 a) V. S. Reuss, B. Obermeier, C. Dingels, H. Frey, *Macromolecules* **2012**, *45*, 4581. b) C. Mangold, F. Wurm, B. Obermeier, H. Frey, *Macromolecules* **2010**, *43*, 8511. c) B. Obermeier, F. R. Wurm, H. Frey, *Macromolecules* **2010**, *43*, 2244.

16 a) A. Natalello, M. Werre, A. Alkan, H. Frey, *Macromolecules* **2013**, *46*, 8467. b) A. Natalello, A. Alkan, P. von Tiedemann, F. R. Wurm, H. Frey, *ACS Macro Lett.* **2014**, *3*, 560. c) E. Grune, T. Johann, M. Appold, C. Wahlen, J. Blankenburg, D. Leibig, A. H. E. Müller, M. Gallei, H. Frey, *Macromolecules* **2018**, *51*, 3527. d) P. von Tiedemann, J. Blankenburg, K. Maciol, T. Johann, A. H. E. Müller, H. Frey, *Macromolecules* **2019**, *52*, 796. e) D. Leibig, A. H. E. Müller, H. Frey, *Macromolecules* **2016**, *49*, 4792. f) D. Leibig, A.-K. Lange, A. Birke, H. Frey, *Macromol. Chem. Phys.* **2017**, *218*, 1600553.

17 T. Johann, D. Leibig, E. Grune, A. H. E. Müller, H. Frey, *Macromolecules* **2019**, *52*, 4545.

18 J.-F. Lutz, *Polym. Chem.* **2010**, *1*, 55.

19 G. Sakellariou, D. Baskaran, N. Hadjichristidis, J. W. Mays, *Macromolecules* **2006**, *39*, 3525.

20 a) E. Harth, B. van Horn, V. Y. Lee, D. S. Germack, C. P. Gonzales, R. D. Miller, C. J. Hawker, *J. Am. Chem. Soc.* **2002**, *124*, 8653. b) O. J. Alley, E. Plunkett, T. S. Kale, X. Guo, G. McClintock, M. Bhupathiraju, B. J. Kirby, D. H. Reich, H. E. Katz, *Macromolecules* **2016**, *49*, 3478. c) K. Jin, J. M. Torkelson, *Macromolecules* **2016**, *49*, 5092.

21 J. Pyun, C. Tang, T. Kowalewski, J. M. J. Fréchet, C. J. Hawker, *Macromolecules* **2005**, *38*, 2674.

22 G. Sakellariou, A. Avgeropoulos, N. Hadjichristidis, J. W. Mays, D. Baskaran, *Polymer* **2009**, *50*, 6202.

23 C. O. Hayes, P.-h. Chen, R. P. Thedford, C. J. Ellison, G. Dong, C. G. Willson, *Macromolecules* **2016**, *49*, 3706.

24 S. Blomberg, S. Ostberg, E. Harth, A. W. Bosman, B. van Horn, C. J. Hawker, *J. Polym. Sci. Part A: Polym. Chem.* **2002**, *40*, 1309.

25 Y. Yu, X. Dong, K. Zhao, J. Cheng, J. Zhang, *Surf. Coat. Technol.* **2010**, *205*, 205.

26 a) E. Drockenmuller, L. Y. T. Li, Y. Du Ryu, E. Harth, T. P. Russell, H.-C. Kim, C. J. Hawker, *J. Polym. Sci. Part A: Polym. Chem.* **2005**, *43*, 1028. b) Y.-H. So, S. F. Hahn, Y. Li, M. T. Reinhard, *J. Polym. Sci. Part A: Polym. Chem.* **2008**, *46*, 2799.

27 a) M. Stamm, *Polymer Surfaces and Interfaces: Characterization, Modification and Applications*; Springer: Berlin, **2008**. b) J. W. Chan, A. Huang, K. E. Uhrich, *Langmuir* **2016**, *32*, 5038.

28 R. Barbey, L. Lavanant, D. Paripovic, N. Schüwer, C. Sugnaux, S. Tugulu, H.-A. Klok, *Chem. Rev.* **2009**, *109*, 5437.

29 a) M. D. Rowe, B. A. G. Hammer, S. G. Boyes, *Macromolecules* **2008**, *41*, 4147. b) M. D. Rowe-Konopacki, S. G. Boyes, *Macromolecules* **2007**, *40*, 879. c) G.-G. Bumbu, G. Kircher, M. Wolkenhauer, R. Berger, J. S. Gutmann, *Macromol. Chem. Phys.* **2004**, *205*, 1713.

30 a) R. Advincula, Q. Zhou, M. Park, S. Wang, J. Mays, G. Sakellariou, S. Pispas, N. Hadjichristidis, *Langmuir* **2002**, *18*, 8672. b) R. P. Quirk, R. T. Mathers, T. Cregger, M. D. Foster, *Macromolecules* **2002**, *35*, 9964.

31 K. Matyjaszewski, H. Dong, W. Jakubowski, J. Pietrasik, A. Kusumo, *Langmuir* **2007**, *23*, 4528.

32 a) K. S. Iyer, B. Zdyrko, H. Malz, J. Pionteck, I. Luzinov, *Macromolecules* **2003**, *36*, 6519. b) M. Henze, D. Mädge, O. Prucker, J. Rühe, *Macromolecules* **2014**, *47*, 2929.

33 Y. Huang, Q. Liu, X. Zhou, S. Perrier, Y. Zhao, *Macromolecules* **2009**, *42*, 5509.

34 N. Tsubokawa, M. Hosoya, K. Yanadori, Y. Sone, *J. Macromol. Sci., Part A: Pure Appl. Chem.* **1990**, *27*, 445.

35 V. S. Wilms, H. Bauer, C. Tonhauser, A.-M. Schilmann, M.-C. Müller, W. Tremel, H. Frey, *Biomacromolecules* **2013**, *14*, 193.

36 P. G. de Gennes, *Macromolecules* **1980**, *13*, 1069.

37 a) R. C. Advincula, *Polymer Brushes: Synthesis, Characterization, Applications*; Wiley-VCH: Weinheim, **2004**. b) G. Fleer, M. A. Cohen Stuart, J. M. H. M. Scheutjens, T. Cosgrove, B. Vincent, *Polymers at Interfaces*; Chapman & Hall: London, **1993**.

38 A. Stamouli, E. Pelletier, V. Koutsos, E. van der Vegte, G. Hadziioannou, *Langmuir* **1996**, *12*, 3221.

39 D. R. M. Williams, *J. Phys. II France* **1993**, *3*, 1313.

40 H. Huang, L. S. Penn, *Macromolecules* **2005**, *38*, 4837.

41 a) R. P. Quirk, G. M. Lizárraga, *Macromolecules* **1998**, *31*, 3424. b) R. P. Quirk, Q. Ge, M. A. Arnould, C. Wesdemiotis, *Macromol. Chem. Phys.* **2001**, *202*, 1761.

42 a) V. E. Meyer, G. G. Lowry, *J. Polym. Sci. Part A: Gen. Pap.* **1965**, *3*, 2843. b) J. Blankenburg, E. Kersten, K. Maciol, M. Wagner, S. Zarbakhsh, H. Frey, *Polym. Chem.* **2019**, *10*, 2863.

43 G. A. Deeter, D. Venkataraman, J. W. Kampf, J. S. Moore, *Macromolecules* **1994**, *27*, 2647.

44 K. Miyake, N. Satomi, S. Sasaki, *Appl. Phys. Lett.* **2006**, *89*, 31925.